Electronic Supplementary Material (ESI) for Nanoscale
This journal is © The Royal Society of Chemistry 2013

Supporting Information

Tuning Electronic and Magnetic Properties of MoO_3 Sheets by Cutting, Hydrogenation, and External Strain: A Computational Investigation

Fengyu Li,[†] Zhongfang Chen[†,*]

Department of Physics, Department of Chemistry, Institute for Functional Nanomaterials, University of Puerto Rico, Rio Piedras Campus, San Juan, PR 00931.

* To whom correspondence should be addressed. Email: zhongfangchen@gmail.com (Z.C.)

[†] University of Puerto Rico

This journal is © The Royal Society of Chemistry 2013

To test the effectiveness of this method, we presented the optimized structure of bulk MoO_3 based on PBE and PBE-D2 approaches, respectively (shown in Figure S1). The PBE yields the two interlayer O-O distances between adjacent layers of 3.335 and 2.855 Å, whereas PBE-D2 predicts the corresponding O-O distances of 3.212 and 2.792 Å, which are more comparable with the experimental values of 3.240 and 2.823 Å. [Kihlborg, L. *Ark. Kemi* **1963**, *21*, 357] The intralayer Mo-O bond lengths within a corrugated plane obtained using PBE and PBE-D2 are similar. Thus PBE-D2 is quantitatively better than PBE when dealing with the weak-bonded layer system.

Table S1. The plane-wave cut off energy test results based on bulk MoO_3, the k-point mesh was choosen as 8 × 6 × 8.

Cut off (eV)	Spin-nonpolarized energy (eV)	Spin polarized energy (eV)	Magnetization (μ_B)
360	-132.031	-132.031	0.0003
400	-132.864	-132.864	0.0003
450	-132.617	-132.617	0.0003
500	-132.647	-132.647	0.0000
550	-132.640	-132.640	0.0000
600	-132.661	-132.661	0.0000

From Table 1, we see that the spin polarized magnetic moment are invariable with different energy cut off, and the energy difference between 500 eV and higher cut-off is less than 0.1 eV, so we choose the cut-off (500 eV) as our computation parameter.

This journal is © The Royal Society of Chemistry 2013

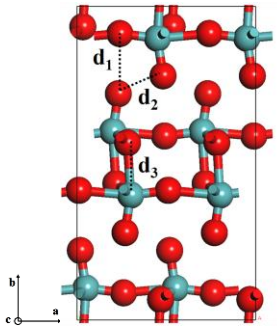

	Exp.	PBE	PBE-D2
a (Å)	3.963	3.974	3.930
b (Å)	13.855	14.508	14.014
c (Å)	3.696	3.720	3.709
d_1 (Å)	3.240	3.335	3.212
d_2 (Å)	2.823	2.855	2.792
d_3 (Å)	2.312	2.457	2.376

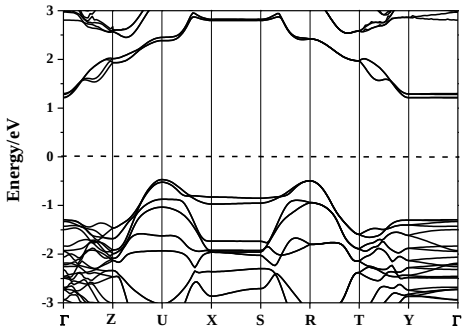

Figure S1. The optimized geometry of bulk MoO_3 based on PBE and PBE-D2, and the band structure from PBE-D2 calculation. The labeled bond length of $\mathbf{d_1}$ and $\mathbf{d_2}$ are the O-O distances between two adjacent layers, $\mathbf{d_3}$ is the Mo-O distance in the same layer along *b*-axis. The cyan and red atoms represent Mo and O atoms, respectively. The experimental data were taken from [Kihlborg, L. *Ark. Kemi* **1963**, *21*, 357]. The bands are plotted along a path connecting high-symmetry points in the irreducible Brillouin zone. The Fermi energy is denoted by a dashed line. The direct band gap is 2.75 eV at gamma point, better than the reported PBE result (2.23 eV),[Sayede, A. D.; Amriou, T.; Pernisek, M.; Khelifa, B.; Mathieu, C. *Chem. Phys.* **2005**, *316*, 72] but slightly lower than the experimental measurement (3.3 eV). [Bouzidi, A.; Benramdane, N.; Tabet-Derranz, H.; Mathieu, C.; Khelifa, B.; Desfeux, R. *Mater. Sci. Eng. B* **2003**, *97*, 5]

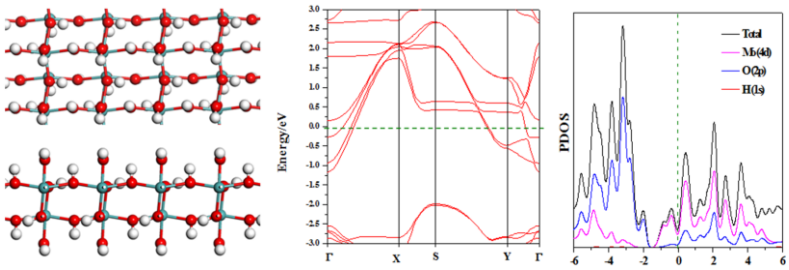

Figure S2. Top and side view of the fully hydrogenated MoO_3 monolayer as well as its band structure and projected density of state with spin-up channel.

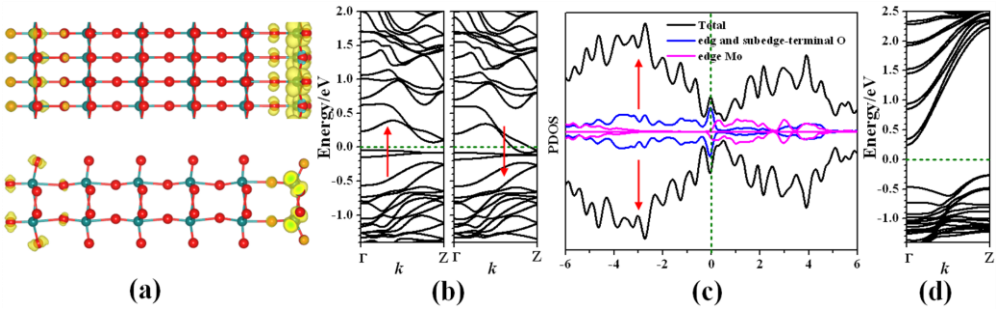

Figure S3. Top and side view of the spatial spin density distribution (a), band structure (b), partial density of states (c) for the second type of 12-*c*-**II** MoO_3 monolayer nanoribbon, and band structure of 12-*c*-**II** MoO_3 monolayer nanoribbon with edge hydrogenated (d).

This journal is © The Royal Society of Chemistry 2013

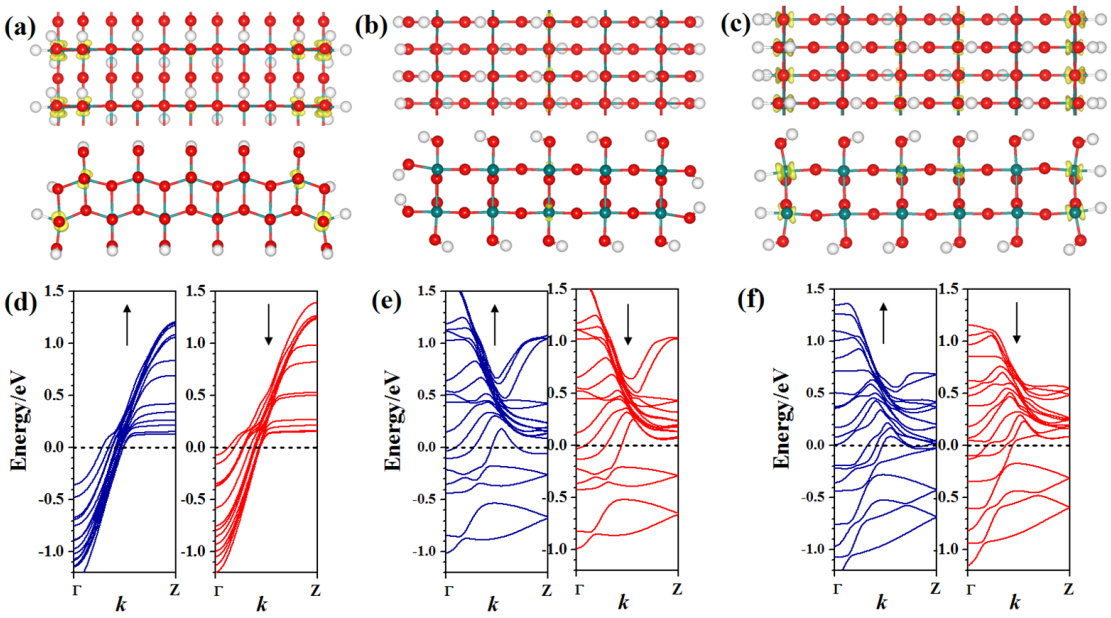

Figure S4. Spatial spin density distribution of *a-11* (a), *c-11*-**I** (b) and *c-11*-**II** (c) nanoribbons where both surface and edge atoms are saturated by H atoms, as well as the corresponding band structures (d), (e) and (f).

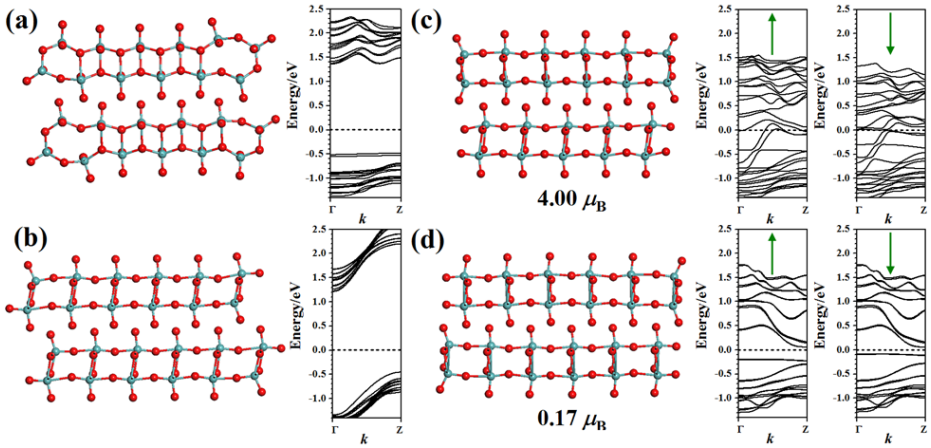

Figure S5. Optimized *a*-12 (a), two types of *c*-12 (b, d) and *c-11*-**I** and *c-11*-**II** combined (c) MoO_3 double-layer nanoribbons, as well as their corresponding band structures.

This journal is © The Royal Society of Chemistry 2013

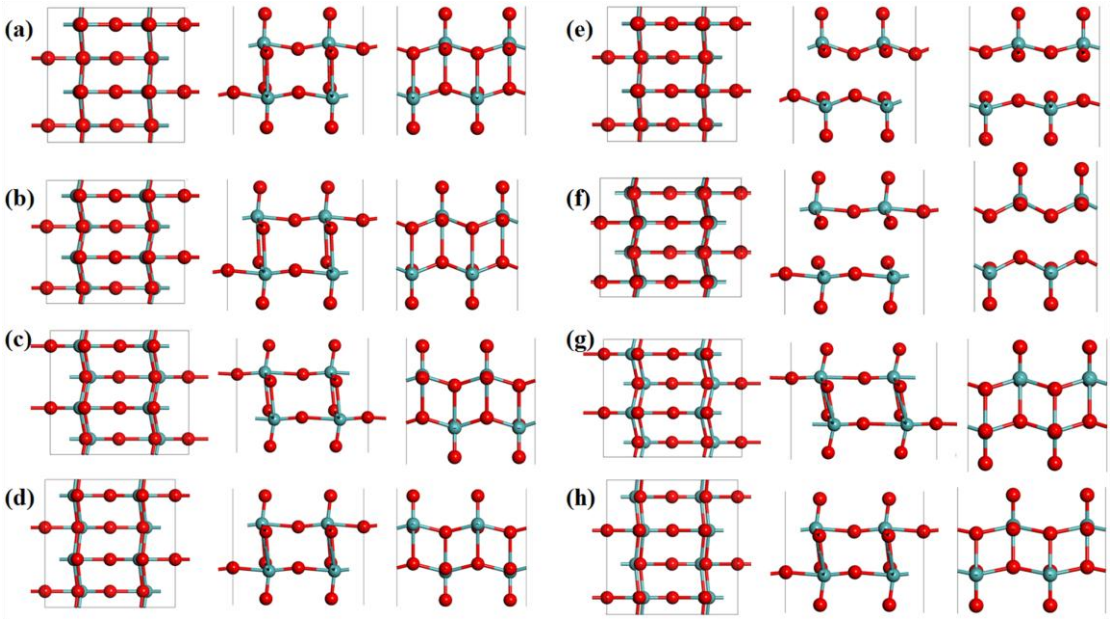

Figure S6. Top (left) and side (right) views of 2D single layer MoO_3 geometries (2×1×2 supercell) with *c*-axis condensed by 5% (a) and 10% (e), stretched by 5% (c) and 10% (g), respectively; with *a*-axis condensed by 5% (b) and 10% (f), stretched by 5% (d) and 10% (h), respectively.

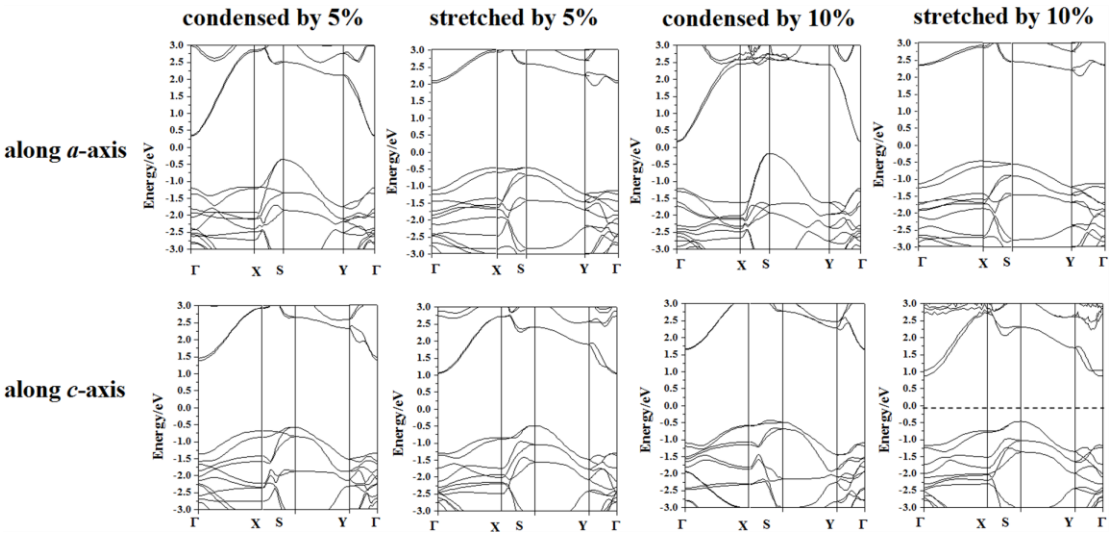

Figure S7. Band structures of MoO_3 monolayer with *a*-axis (upper panel) and *c*-axis (lower panel) condensed and stretched by 5% and 10%, respectively.

This journal is © The Royal Society of Chemistry 2013

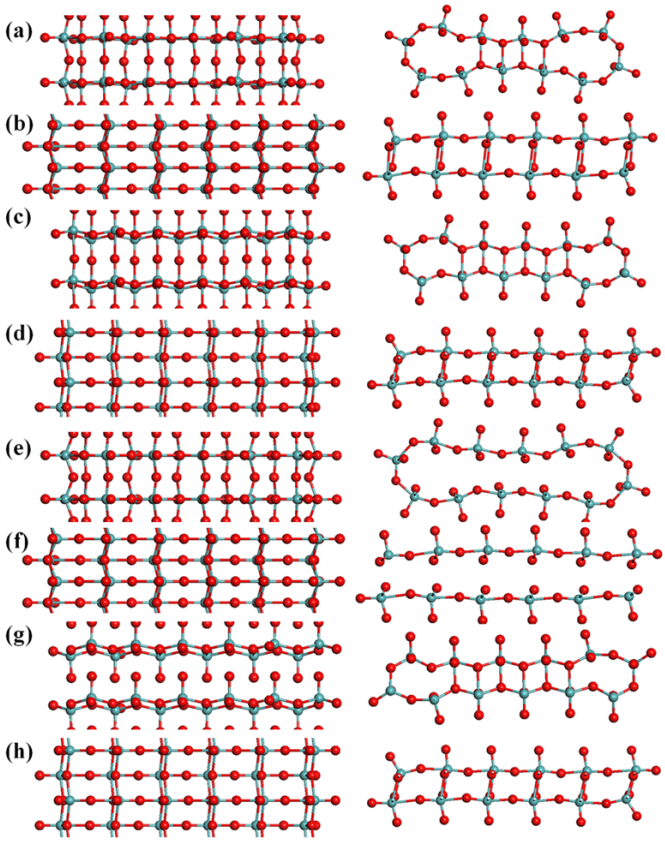

Figure S8. Top (left) and side (right) views of 1D single-layer MoO_3 *a-12* nanoribbon condensed by 5% (a) and 10% (e), stretched by 5% (c) and 10% (g) along *a*-axis, respectively; *c-12* NR condensed by 5% (b) and 10% (f), stretched by 5% (d) and 10% (h) along *c*-axis, respectively.

This journal is © The Royal Society of Chemistry 2013

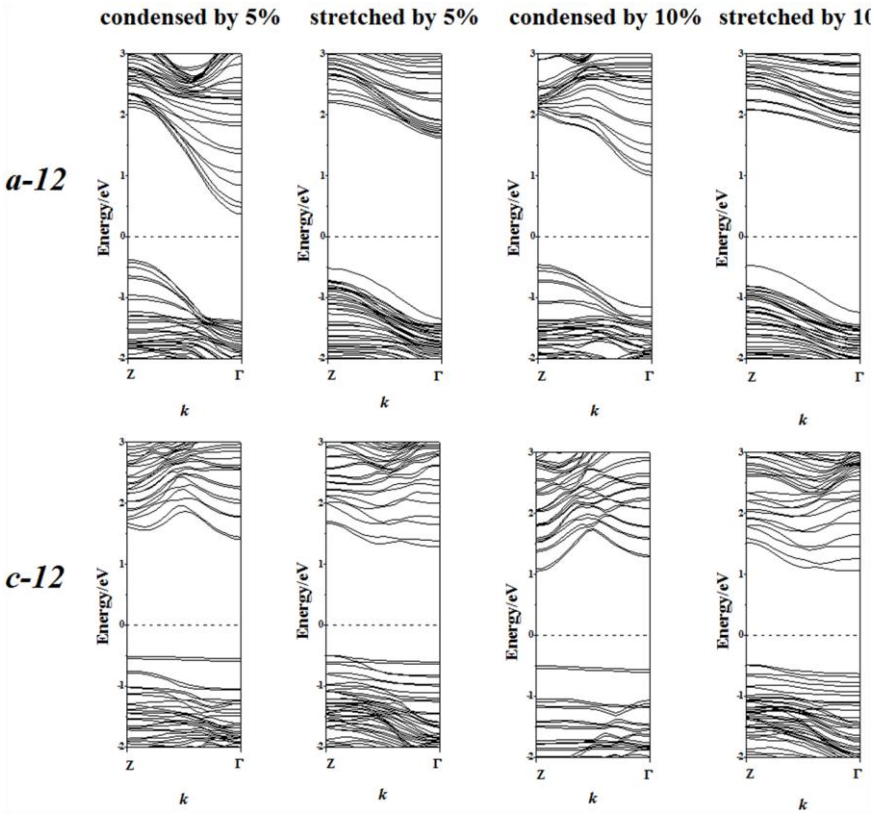

Figure S9. Band structures of *a-12* (upper panel) and *c-12* (lower panel) MoO_3 single-layer nanoribbons with *c*-axis and *a*-axis condensed and stretched by 5% and 10%, respectively.